UCRL-JC-132068
PREPRINT

Atomistic Simulations for Multiscale Modeling in bcc Metals

J.A. Moriarty
W. Xu
P. Soderlind
J. Belak
L.H. Yang
J. Zhu

This paper was prepared for submittal to the
Symposium on Multiscale Modeling of Deformation and Fracture
Pullman, WA
September 28-29, 1998

September 25, 1998

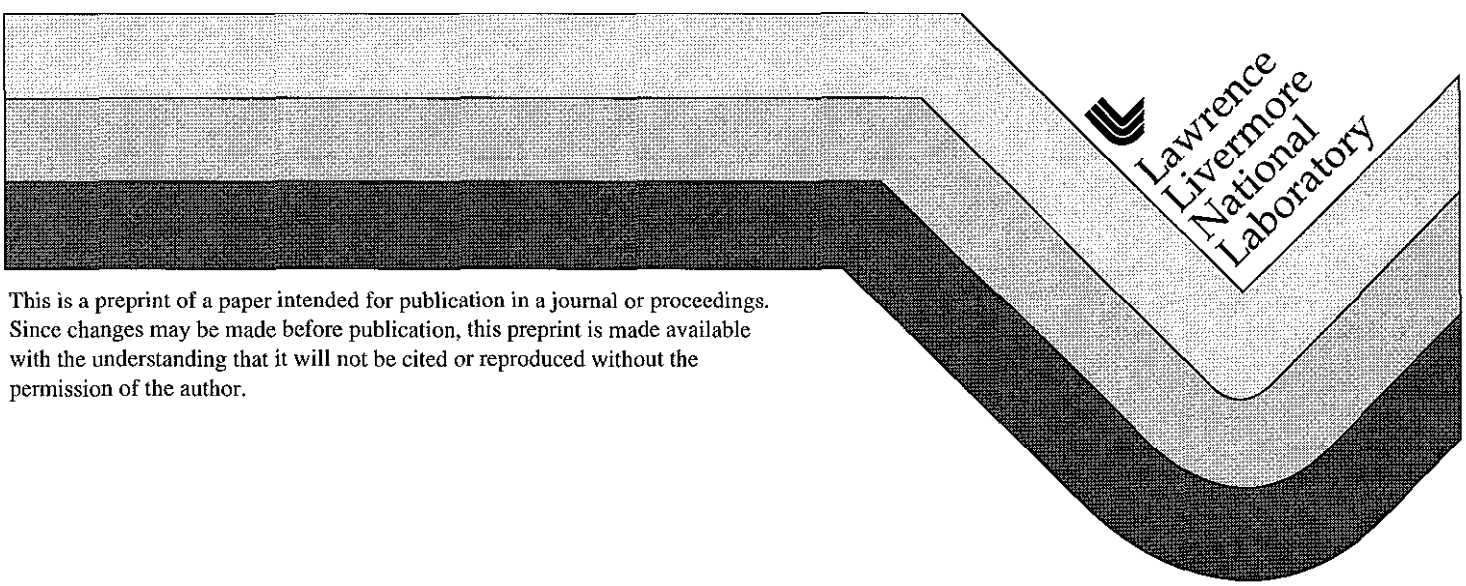

Atomistic Simulations for Multiscale Modeling in bcc Metals

John A. Moriarty, Wei Xu[†], Per Söderlind, James Belak,
Lin H. Yang, and Jing Zhu[‡]

Lawrence Livermore National Laboratory
University of California
Livermore, CA 94551

ABSTRACT

Quantum-based atomistic simulations are being used to study fundamental deformation and defect properties relevant to the multiscale modeling of plasticity in bcc metals at both ambient and extreme conditions. *Ab initio* electronic-structure calculations on the elastic and ideal-strength properties of Ta and Mo help constrain and validate many-body interatomic potentials used to study grain boundaries and dislocations. The predicted $\Sigma 5$ (310)[100] grain boundary structure for Mo has recently been confirmed in HREM measurements. The core structure, γ surfaces, Peierls stress, and kink-pair formation energies associated with the motion of a/2<111> screw dislocations in Ta and Mo have also been calculated. Dislocation mobility and dislocation junction formation and breaking are currently under investigation.

[†]Present address: Synopsys, Inc., 700 East Middlefield Rd., Mountain View, CA 94043
[‡]Present address: Visto Corp., 1937 Landings Dr., Mountain View, CA 94043

I. INTRODUCTION

Mechanical properties such as plastic flow in metals depend on phenomena which occur at multiple length scales ranging from atomistic to continuum. With the recent and continuing expansion of large-scale computing capabilities, there has been a growing interest in attempting to bridge the length scales and address such properties from a fundamental perspective (e.g., Yip, 1996). At Lawrence Livermore National Laboratory (LLNL) we are developing a comprehensive multiscale modeling program, whose initial goal is a rigorous treatment of plastic flow in bcc transition metals at both ambient and extreme conditions. Here the role of atomistic simulations is to provide an accurate description of deformation and defect energetics as input into larger length scale simulations such as 3D (three dimensional) dislocation dynamics at the mircroscale (e.g., Tang et al., 1998). In the present work, state-of-the-art electronic-structure and interatomic-potential methods are being used to study a wide range of relevant, fundamental properties of bcc metals, including elastic moduli, ideal shear strength, and the atomic structure and energetics of grain boundaries and dislocations. Two metals of special interest in this regard are tantalum (Ta) and molybdenum (Mo).

In the case of Ta, a comprehensive set of *ab initio* electronic-structure calculations have been performed recently on the basic structural, vibrational, and mechanical properties of the bulk metal in the 0-10 Mbar pressure range (Söderlind and Moriarty, 1998). Such results can be combined with rigorous generalized pseudopotential theory (GPT) to develop corresponding model-GPT (MGPT) interatomic potentials (Moriarty, 1990; 1994) suitable for realistic atomistic simulations, and this has been done in both Ta and Mo. Many-body angular forces, which are accounted for in the MGPT through explicit three- and four-ion potentials, are generally important to the structural and mechanical properties of bcc transition metals. This is revealed, for example, in the atomic stucture of grain boundaries. In this regard, the $\Sigma 5$ (310)[100] boundary has been calculated in both Mo and Ta for comparison with concurrent high-resolution electron microscopy (HREM) measurements, as an additional validation test for the MGPT potentials. With regard to dislocations, our previous studies on Mo (Xu and Moriarty, 1996; 1998) have now been extended to Ta and generalized in scope. In the present work, we have investigated the core structure, the generalized stacking-fault (γ) energy surfaces, the Peierls stress, and kink-pair formation energies associated with the motion of a/2<111> screw dislocations on the primary {110} and {112} slip planes in these metals. In addition, we are calculating kink-pair migration and activation energies, including both their stress and orientation dependence, to obtain

full dislocation mobilities. These latter quantities control the low-temperature plasticity in bcc metals and are essential input for microscale dislocation-dynamics simulations (Tang et al, 1998). We are also studying dislocation-dislocation interactions in an attempt to accurately model junction formation and breaking, which are fundamental to the description of strain hardening at the microscale.

II. THEORETICAL METHODS

The present atomistic simulation methods are based on the modern density-functional theory of quantum mechanics, as expressed in the well known local-density approximation (LDA) to the treatment of exchange and correlation or in recent extensions such as the generalized-gradient approximation. The focus of these methods is on obtaining the total energy of the electron-ion system as a functional of the electron density for a given configuration of the ions. For metals, two general strategies can be followed. The first and most common is to exploit the symmetry of the ion configuration and seek a direct numerical solution of the LDA equations. This leads to the usual *ab initio* electronic structure techniques of condensed matter theory, such as the full-potential, linear muffin-tin orbital (FP-LMTO) method used in the present work. These techniques are chemically very robust, but are order-N^3 scaling with respect to the number of independent ion positions which can be treated. Thus they are practical only for relatively high symmetry situations. An alternate and complementary strategy is to cast the electronic structure problem into a form in which small quantities can be defined and used as a basis for rigorous expansions of the electron density and total energy. In real space, this leads to expansion of the total energy in terms of *ab initio* multi-ion interatomic potentials. Such techniques are order-N scaling and structurally very robust, but require truncation of the interatomic-potential series at low order to be tractable.

Within the LDA framework, generalized pseudopotential theory (GPT) provides a fundamental basis for *ab initio* interatomic potentials in elemental transition metals (Moriarty, 1988). For an elemental bulk metal, the GPT provides a rigorous expansion of the total energy in the form

$$E_{tot}(R_1 \ldots R_N) = E_{vol}(\Omega) + \frac{1}{2}{\sum_{i,j}}' v_2(ij;\Omega) + \frac{1}{6}{\sum_{i,j,k}}' v_3(ijk;\Omega) + \frac{1}{24}{\sum_{i,j,k,l}}' v_4(ijkl;\Omega) \quad , \qquad (1)$$

where $R_1 ... R_N$ denotes the positions of the N ions in the metal, Ω is the atomic volume, and the prime on each sum over ion positions excludes all self-interaction terms where two indices are equal. The leading volume term in this expansion, E_{vol}, as well as the two-, three-, and four-ion interatomic potentials, v_2, v_3, and v_4, are volume dependent, *but structure independent* quantities and thus *transferable* to all bulk ion configurations, either ordered or disordered. This includes all structural phases as well as the deformed solid and the imperfect bulk solid with either point or extended defects present. The angular-force multi-ion potentials v_3 and v_4 in Eq. (1) reflect contributions from partially-filled *d* bands and are generally important for central transition metals. In the full GPT, however, these potentials are long-ranged, nonanalytic, and multidimensional functions, so that v_3 and v_4 cannot be readily tabulated for application purposes. This has led to the development of a simplified model GPT or MGPT for bcc transition metals (Moriarty, 1990; 1994). In the MGPT, the multi-ion potentials are systematically approximated by introducing canonical *d* bands and other simplifications to achieve short-ranged, analytic forms, which can then be applied to both static and dynamic simulations. To compensate for the approximations introduced, a limited amount of parameterization is allowed in which the coefficients of the modeled potential contributions are constrained by external experimental or *ab initio* theoretical data. The principal data used in this regard are the elastic moduli, the vacancy formation energy, and the zero-temperature equation of state. Useful MGPT potentials have been so determined for Mo over a wide volume range (Moriarty, 1994) and this metal has served as the prototype for many applications. Preliminary MGPT potentials have also been determined for Ta in the 0-10 Mbar regime. Implementation of the MGPT potentials can be accomplished in static simulations with standard energy-minimization techniques and in dynamic simulations with either molecular dynamics (MD) or Monte Carlo methods.

III. MECHANICAL PROPERTIES

We now discuss the application of the FP-LMTO electronic-structure and MGPT interatomic-potential methods to the calculation of important mechanical properties of bcc metals. In this regard, our interest is in both fundamental deformation properties such as elastic moduli and ideal shear strength and in important defect properties, including the structure and energetics of grain boundaries and dislocations. These quantities are expected to underpin the rigorous multiscale modeling of macroscopic mechanical properties related to plasticity in bcc metals such as the yield strength.

A. Elastic moduli and ideal shear strength

Ab initio elastic moduli in bcc transition metals can be calculated from the FP-LMTO method in terms of the bulk modulus and the two shear constants C' and C_{44}. The bulk modulus is readily obtained from the zero-temperature equation of state, while the calculation of the shear elastic constants involves computing the change in total energy at constant volume for appropriate small applied strains. This approach has been carried out in detail for the case of bcc Ta over the 0-10 Mbar pressure range (Söderlind and Moriarty, 1998). The predicted results for C' and C_{44} are plotted in Fig. 1. The bulk and shear moduli are calculated to be everywhere positive and show smooth monotonic behavior as a function of pressure. This demonstrates full mechanical stability for bcc Ta over the entire 0-10 Mbar pressure range. In addition, at zero pressure the calculated elastic moduli are in good agreement with experiment. It is also noteworthy that under compression and C_{44} increases more rapidly with pressure than C'. This indicates that Ta is increasingly anisotropic at high pressure, and the anisotropy ratio $A = C_{44}/ C'$ increases from 1.58 at zero pressure to a value of 2.22 at 10 Mbar. Although such an increase is somewhat counterintuitive, it is not uncommon in metals. Diamond-anvil-cell experiments to measure the high-pressure elastic moduli of Ta are currently in progress (Yoo, 1998).

In addition to their importance in developing MGPT potentials, the FP-LMTO high-pressure elastic moduli for bcc Ta have also been used to analyze the assumed pressure dependence of the well known Steinberg-Guinan (SG) strength model (Steinberg et al., 1980) for polycrystalline Ta and to establish approximate lower and upper bounds on the high-pressure yield strength of the metal (Söderlind and Moriarty, 1998). The lower bound is inspired by the SG model itself. This model assumes that the yield stress of a metal scales linearly with its average shear modulus. The pressure dependent shear modulus appropriate to the polycrystal can be calculated from our *ab initio* results as a simple Voigt average of the two bcc shear elastic moduli:

$$G_V(P) = [2C'(P) + 3C_{44}(P)]/5 \quad . \tag{2}$$

This result combined with the SG model implies a scaling relation for the yield strength Y in the form

$$Y(P) = Y_0 G_V(P)/G_V(0) \quad , \tag{3}$$

where Y_0 is the observed ambient value (0.77 GPa for pure Ta). The available experimental evidence (Steinberg et al., 1980; Weir et al., 1998), however, indicates that the actual yield strength of a metal increases faster with pressure than does the shear modulus. This suggests that at high pressure Eq. (3) is, in fact, a lower bound.

A corresponding upper bound to the yield strength can be established by considering the ideal theoretical shear strength of the perfect bcc crystal, in the complete absence on any dislocations or grain boundaries. A specific procedure to calculate this quantity for real materials has been suggested and applied to fcc and bcc metals by Paxton, et al. (1991). The ideal shear strength is defined to be the critical stress separating elastic and plastic deformation under the continuous homogeneous shearing of the perfect crystal into itself via the observed twinning mode. For bcc metals, this mode is specified by the shear direction $\eta = [\bar{1}\,\bar{1}\,1]$ and the normal plane $\mathbf{K} = (112)$. Neglecting any relaxation normal to **K**, which is indeed small, the atomic positions during the deformation can be analytically related to the amount of shear. The calculation may be carried out entirely using a single atom per unit cell and periodic boundary conditions, which allows *ab initio* computation of the ideal strength by the FP-LMTO technique. The result for Ta is plotted in Fig 2 over the 0-10 Mbar pressure range and compared with the lower bound given by Eq. (3). Note that the two bounds remain within an order of magnitude of each other over the whole 0-10 Mbar range. Diamond-anvil-cell experiments to measure the high-pressure yield strength of Ta have very recently been performed up to 2 Mbar and the data are indeed found to be within these limits (Weir et al., 1998).

B. Grain boundary and dislocation-core structure

The calculation of a wide range of point and extended defects and their interactions in bcc transition metals is possible with the MGPT potentials. Problems considered to date are the formation and migration of vacancies and self-interstitials, the atomic structure of grain boundaries, generalized-stacking-fault or γ energy surfaces, the core structure and motion of rigid screw and edge dislocations, and the formation of dislocation kinks. A few of the simplier problems, such as the vacancy formation energy, the structure of high-symmetry grain boundaries, and the γ surface can also be readily addressed with *ab initio* electronic structure methods, and this is important with regard to the further development and validation of the potentials. The role of interatomic potentials becomes most important in the case of dislocations, where, for example, up to 100,000 atoms are required to model the formation and motion of a double kink.

Grain boundaries are important in the present context not only because of their possible role in polycrystalline plasticity but also because their detailed atomic structrure can be studied using high-resolution transmission electron microscopy (HREM). The latter provides a clear means of testing the ability of specific interatomic potentials to predict the structure of an extended defect. Such a combined experimental and theoretical study was first performed in the case of bcc niobium (Nb) for the Σ5 (310)[001] symmetric tilt boundary (Campbell et al., 1993). A mirror symmetric structure was found experimentally and also predicted theoretically using multi-ion MGPT potentials. Simple radial-force embedded-atom-method (EAM) (Johnson and Oh, 1989) or Finnis-Sinclair (FS) (Ackland and Thetford, 1987) potentials, on the other hand, incorrectly yielded symmetry breaking structures. This serves to underscore the importance of the angular-force contributions contained in the MGPT treatment. More recently, attention has turned to the cases of Mo and Ta. Unlike Nb, in both of these metals multi-ion MGPT potentials predict a breaking of the mirror symmetry for the Σ5 (310)[001] boundary, as shown in Fig. 3. In the case of Mo, recent *ab initio* LDA electronic-structure calculations (Elsässer et al., 1998) predict the same mirror-symmetry breaking, as do previous fourth-moment tight-binding calculations (Marinopoulos, 1995), which also accommodate angular-force interactions. Radial-force FS potentials, on the other hand, predict a mirror-symmetric structure (Bacia et al., 1997). While the initial experimental HREM measurements (Bacia et al., 1997) on this boundary in Mo were inconclusive, recent measurements (Campell et al., 1998) have confirmed the mirror-symmetry breaking. Experimental studies on Ta are currently in progress (Campbell, 1998).

The possible core configurations of a/2<111> screw dislocations in bcc Mo and Ta have also been carefully studied with the MGPT potentials Two mechanically stable types of configurations are found: the so-called "easy" and "hard" cores, obtained with the Burgers vector **b** either parallel or anti-parallel to the dislocation line. Both configurations are nonplanar in character and possess three-fold symmetry. The easy core is the stable ground state and is spread out on three {110} planes in <112> directions, as shown in Fig. 4a for Ta. Because there are six possible <112> directions here, the easy core can have either of two orientations and is thus doubly degenerate. The two orientations physically correspond to positive (p) and negative (n) polarizations of the core. The higher-energy and higher-symmetry hard core, on the other hand, is more compact without any directional spreadout. This configuration is nondegenerate with a calculated formation energy that is respectively 0.24 and 0.14 eV/b higher than that of the stable easy core in Mo and Ta.

It is also interesting to compare and constrast the core structures predicted by the angular-force MGPT potentials with those predicted by simplier radial-force potentials. In the case of Mo, the same type of polarized, doubly degenerate easy-core ground state is found both with empirical pair potentials (Vitek, 1974) and with many-body, but still radial-force, FS potentials (Duesbery and Vitek, 1998). In either case, however, the corresponding nondegenerate hard-core excited state is unstable. In addition, there may be significant quantitative differences in the easy-core structure, as is suggested, for example, by the higher γ surface energies obtained with the MGPT potentials than the FS potentials (Xu and Moriarty, 1998). In the case of Ta, unlike Mo, qualitatively different ground-state structures are predicted with the MGPT and FS potentials. While a degenerate easy-core structure is maintained with the MGPT, the FS potential for Ta yields an isotropic, nondegenerate structure without directional speadout (Duesbery and Vitek, 1998). To help validate the MGPT Ta results, we have also performed *ab initio* FP-LMTO calculations of high-symmetry portions of the {110} and {211} γ surfaces for direct quantitative comparison with MGPT predictions. The periodic γ energy surface is defined and calculated by the continuous relative displacement of two semi-infinite half blocks of crystal across the given surface, allowing atomic relaxation only in the direction normal to the surface (Vitek, 1974). The full MGPT-calculated {110} and {211} γ surfaces for Ta are displayed in Fig. 5. High-symmetry lines along the <110> and <111> directions on the {211} surface are compared with *ab initio* FP-LMTO calculations in Fig. 6. The agreement is seen to be quite good, especially in the <111> direction.

C. Dislocation motion and kinks

In addition to their core structure, the motion of the a/2<111> screw dislocations is of fundamental interest. The minimum or Peierls stress to move a rigid, straight screw dislocation in the bcc lattice depends strongly on the orientation of the applied stress (Duesbery, 1984). As a step towards determining the full orientation dependence of the Peierls stress in Mo, the application of pure shear or glide stresses on the relaxed easy-core dislocation has been examined with MGPT potentials (Xu and Moriarty, 1998). In general, only two pure shear stress components, σ_{zx} and σ_{zy}, can generate a nonzero glide force (Peach-Koehler force) on an a/2<111> screw dislocation whose Burgers vector is along the z axis. These are stresses oriented along the <111> direction on the {112} and {110} slip planes, respectively. In units of the shear modulus G_{111}, the corresponding Peierls stresses for Mo are found to be 0.025 and 0.045, respectively. In both cases the

actual motion of the screw dislocation is on a {110} plane. Preliminary MGPT results for Ta show similar behavior, with calculated Peierls stresses of $\sigma_{zx} = 0.022$ and $\sigma_{zy} = 0.030$. All of these stress values are, of course, very large relative to what one envisages for a highly mobile dislocation. For this reason, it is believed that the formation of mobile kinks on the dislocation line is essential to activate the motion of bcc screw dislocations at low temperature.

One is thus led to consider kink-pair formation on an a/2<111> screw dislocation in bcc transition metals. An elementary kink can be formed by displacing a segment of length R_k parallel to the dislocation line on a {110} or {112} slip plane to the next available core center. The left and right kinks will elastically attract one another, so the kink will be unstable against collapse if R_k is less than some critical distance. In Mo this distance is predicted to be about 4b (10.9 Å) for kinks formed on a {110} slip plane, on the basis of MGPT calculations (Xu and Moriarty, 1998). For larger kink lengths a stable kink pair is formed. The corresponding kink formation energy for the fully relaxed Mo kink pair as function of R_k is plotted in Fig. 7. The result has an interesting two plateau structure. For $4b < R_k < 15b$, the formation energy is near 0.7 eV/kink. In this regime the left- and right-hand kinks are strongly interacting, but there is apparently a sufficiently large migration barrier to stablize the kink pair without an applied stress. The details of this barrier are currently under investigation. For large kink lengths $R_k > 15b$, on the other hand, the kinks become weakly interacting and the formation energy rises to an asymptotic value of about 1.0 eV/kink or 2.0 eV per kink pair.

The above example represents a pure kink pair where the three segments of screw dislocation all have the same orientation (p or n) of the doubly degenerate easy-core configuration. It is also possible to have mixed kink pairs involving individual p and n segments. In addition, bcc symmetry does not require the left- and right-hand kinks to be degenerate and in general they will have different formation energies even if the orientation of the screw dislocation segments from which they are formed is the same (Bulatov et al., 1997). Taking into account the two possible orientations of the core, there are consequently six distinct kinks and three distinct kink pairs that can be formed (Duesbery, 1983). The latter can be denoted as p-p-p (degenerate with n-n-n), p-n-p and n-p-n. The first is the pure kink pair considered in Fig. 7. The latter two mixed kink pairs can have higher or lower formation energies on a given slip plane, and MGPT calculations on Ta indicate that the lowest formation energy will be of an n-p-n type on both the {110} and {112} slip planes. On the {110} planes, the preliminary calculated n-p-n, p-p-p, and p-n-p

formation energies are 0.70, 0.99 and 1.44 eV, respectively. On the {211} planes, the formation energies are up to 1.0 eV higher, due in part to the larger required kink height. It is also possible to have a similar n-p-n or p-n-p changes in orientation along straight screw segments themselves. Such an object has been called a soliton. The MGPT-calculated soliton formation energies are 0.65 and 0.52 eV, respectively, in Mo and Ta. Taking the possiblity of solitons into account, the multiplicity of possible kinks and kink pairs grows even larger.

The much higher kink-pair formation energies on {211} planes begs the question of how slip actually occurs on these planes, as is experimentally observed in bcc metals. A possible explanation is depicted schematically in Fig. 8. Consider the lowest-energy migration path for an a/2<111> screw dislocation moving via kink-pair formation at very low stress. If a dislocation at the bottom of the figure initially has an n-type polarization, it can move at lowest energy cost by forming an n-p-n mixed kink on the (101) plane. Moving the dislocation one spacing, however, rotates it by 60 degrees effectively converting its polarization to p-type with respect to motion in the same direction. To continue moving on the same plane would require forming a higher energy p-p-p kink (or an even higher energy p-n-p kink). However, by next moving on an (011) plane the dislocation can again proceed by forming the lowest energy n-p-n type kink. As can be inferred from Fig. 8, the lowest energy path through the lattice is thus a zig-zag one which macroscopically appears as motion on a (112) plane. At higher levels of stress, the corresponding stress-dependent kink activation energies must be considered and the situation can change. For example, at high enough stress levels one would expect to be able to bias the motion along {110} planes. Calculation of the relevant kink activation energies as a function of stress is currently in progress. In this context, we are also investigating the role of such kink-pair processes to dislocation mobility and to the formation and breaking of dislocation junctions.

IV. CONCLUSIONS

In this paper we have discussed recent progress in the atomistic simulation of the fundamental deformation and defect properties of prototype bcc transition metals using FP-LMTO electronic-structure and MGPT interatomic-potential techniques. The *ab initio* FP-LMTO method can provide reliable results on elastic moduli, ideal shear strength, and high-symmetry features of the γ surfaces, as well as basic bulk properties of the metal. These calculations not only underpin the fundamental description of mechanical properties as a

whole in metals, but they also provide valuable data to help validate interatomic potentials to treat extended defects. In this regard, complementary MGPT potentials can provide the necessary input on the atomic structure and energetics of grain boundaries and dislocations to bridge the gap between the atomic scale and higher length scales. This linkage is essential to the rigorous multiscale modeling of macroscopic mechanical properties such as stength and plastic flow.

ACKNOWLEDGEMENTS

This work was performed under the auspices of the U.S. Department of Energy by the Lawrence Livermore National Laboratory under contract number W-7405-ENG-48.

REFERENCES

Ackland, G. J. and Thetford, R., Philos. Mag. A, **56** (1987) 15.

Bacia, M., Morillo, J., Penisson, J. M., and Pontikis, V., Philos. Mag. A, **76** (1997) 945.

Bulatov, V., Justo, J. F., Cai, W., and Yip, S., Phys. Rev. Lett., **79** (1997) 5042.

Campbell, G. H., Foiles, S. M., Gumbsch, P., Rühle, M., and King, W. E., Phys. Rev. Lett., **70** (1993) 449.

Campbell, G. H. (private communication, 1998).

Campbell, G. H., Belak, J., and Moriarty, J. A. (to be published, 1998).

Duesbery, M. S., Acta Metall., **31** (1983) 1747.

Duesbery, M. S., Proc. R. Soc. London A, **392** (1984) 145.

Duesbery, M. S. and Vitek, V., Acta Mater., **46** (1998) 1481.

Elsässer, C., Beck, O., Ochs, T., and Meyer, B., Mat. Res. Soc. Symp. Proc., **492** (1998) 121.

Finnis, M. W. and Sinclair, J. E., Philos. Mag. A, **50** (1984) 45.

Johnson, R. A. and Oh, D. J., J. Mater. Res., **4** (1989) 1195.

Marinopoulos, A. G., Vitek, V., and Carlsson, A. E., Philos. Mag. A, **72** (1995) 1311.

Moriarty, J. A., Phys. Rev. B, **38** (1988) 3199.

Moriarty, J. A., Phys. Rev. B, **42** (1990) 1609.

Moriarty, J. A., Phys. Rev. B, **49** (1994) 12 431.

Paxton, A. T., Gumbsch, P., and Methfessel, M., Philos. Mag. Lett., **63** (1991) 267.

Söderlind, P. and Moriarty, J. A., Phys. Rev. B, **57** (1998) 10 340.

Steinberg, D. J., Cochran, S. G., Guinan, M. W., J. Appl. Phys., **51** (1980) 1498.

Tang, M., Kubin, L. P., and Canova, G. R., Acta Mater., **46** (1998), 3221.

Vitek, V., Cryst. Lattice Defects, **5** (1974) 1.

Weir, S. T., Akella, J., Ruddle, C., Goodwin, T., and Hsiung, L., Phys. Rev. B, **58** (1998, in press).

Xu, W. and Moriarty, J. A., Phys. Rev. B, **54** (1996) 6941.

Xu, W. and Moriarty, J. A., Comput. Mat. Sci., **9** (1998) 348.

Yip, S. (Ed), Journal of Computer-Aided Materials Design, Vol. 3, proceedings of the workshop on Modeling Industrial Materials: Connecting Atomistic and Continuum Scales, ESCOM, Leiden, 1996.

Yoo, C.-S. (private communication, 1998).

FIGURE CAPTIONS

Fig. 1. High-pressure shear elastic moduli in bcc Ta, as predicted by *ab initio* FP-LMTO calculations (Söderlind and Moriarty, 1998).

Fig. 2. Approximate upper and lower bounds on the yield strength of Ta obtained from *ab initio* FP-LMTO calculations (Söderlind and Moriarty, 1998), as discussed in the text.

Fig. 3. Atomic structure of the Σ5 (310)[001] grain boundary in selected bcc metals, as obtained from MD simulations using multi-ion MGPT potentials. Left panel: Nb; central panel: Mo; right panel: Ta.

Fig. 4. Predicted ground-state core structures of a/2<111> screw dislocations in bcc Ta, as obtained from the present multi-ion, angular-force MGPT potentials (a) and from simple radial-force FS potentials (Duesbery and Vitek, 1998) (b). In the differential-displacement representation shown, the arrow joining two atoms is proportional to the perpendicular relative displacement of the two atoms along the dislocation line.

Fig. 5. Calculated γ surfaces in Ta from multi-ion MGPT potentials. (a) (110) surface; (b) (211) surface.

Fig. 6. Computed (211) γ surface in Ta along symmetry lines, as obtained from *ab initio* FP-LMTO calculations and from multi-ion MGPT potentials. (a) the $[0\bar{1}1]$ direction; (b) $[\bar{1}11]$ the direction.

Fig. 7. Left: schematic representation of a double kink of length R_k formed on an a/2<111> screw dislocation line. Right: double-kink formation energy for a pure (p-p-p) dislocation configuation formed on a {110} slip plane in bcc Mo, as obtained from multi-ion MGPT simulations (Xu and Moriarty, 1998).

Fig. 8. Schematic representation of screw dislocation motion through a bcc lattice at low levels of stress via the formation and migration of mixed-character (n-p-n) double kinks, as discussed in the text.

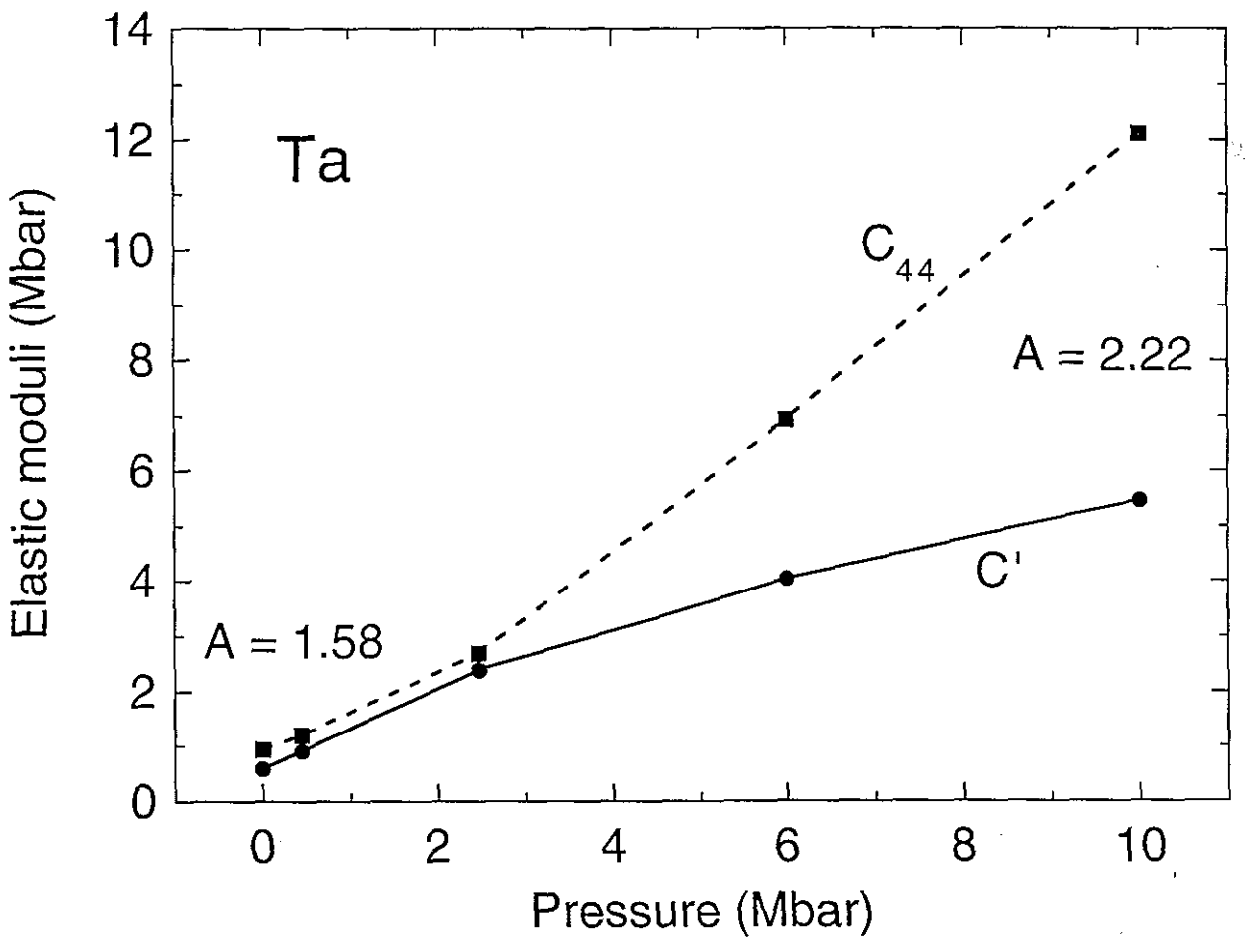
Ta
C_{44}
A = 2.22
C'
A = 1.58
Elastic moduli (Mbar)
Pressure (Mbar)
0
2
4
6
8
10
12
14

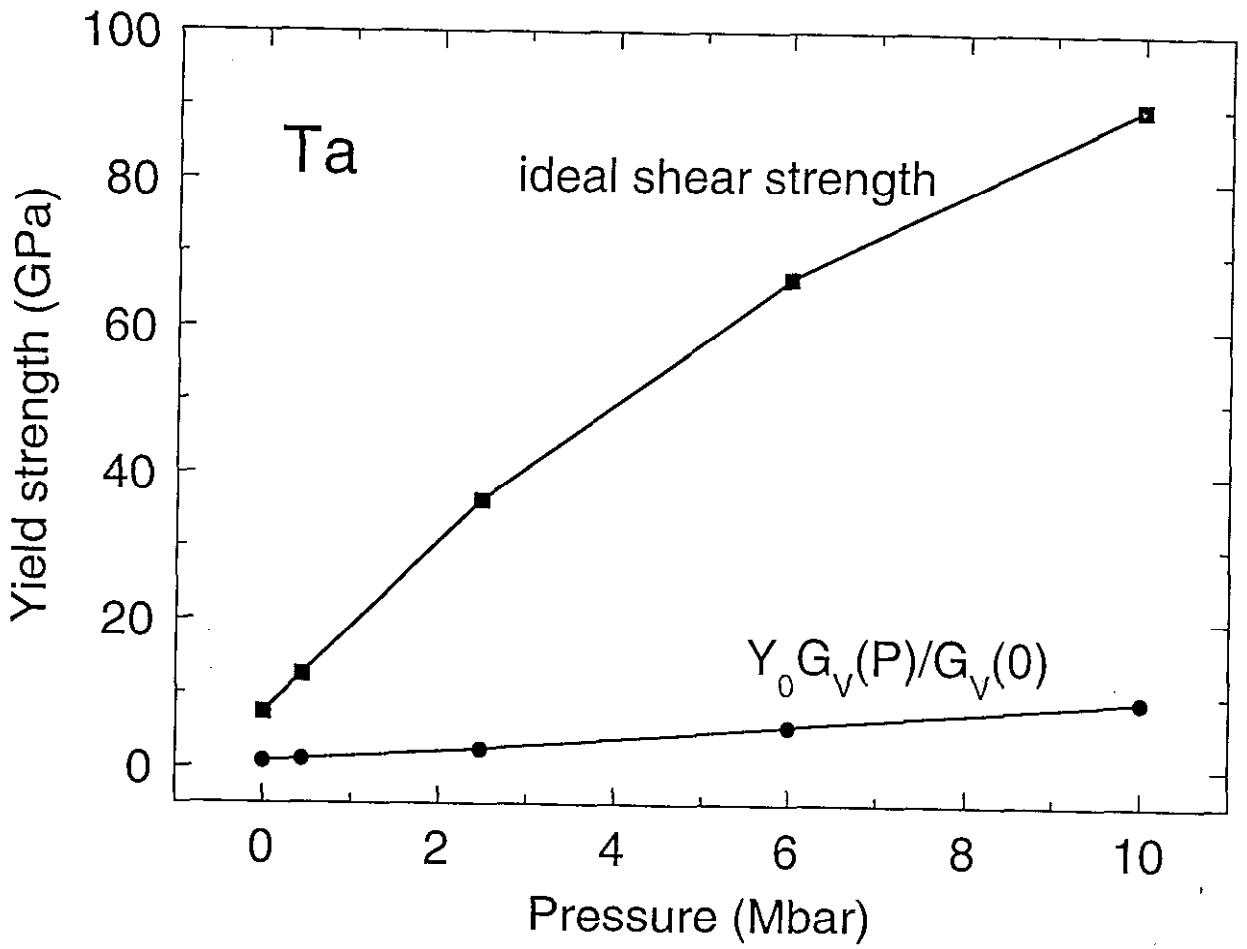
Ta
ideal shear strength
$Y_0 G_V(P)/G_V(0)$
Yield strength (GPa)
Pressure (Mbar)
0
20
40
60
80
100
0
2
4
6
8
10

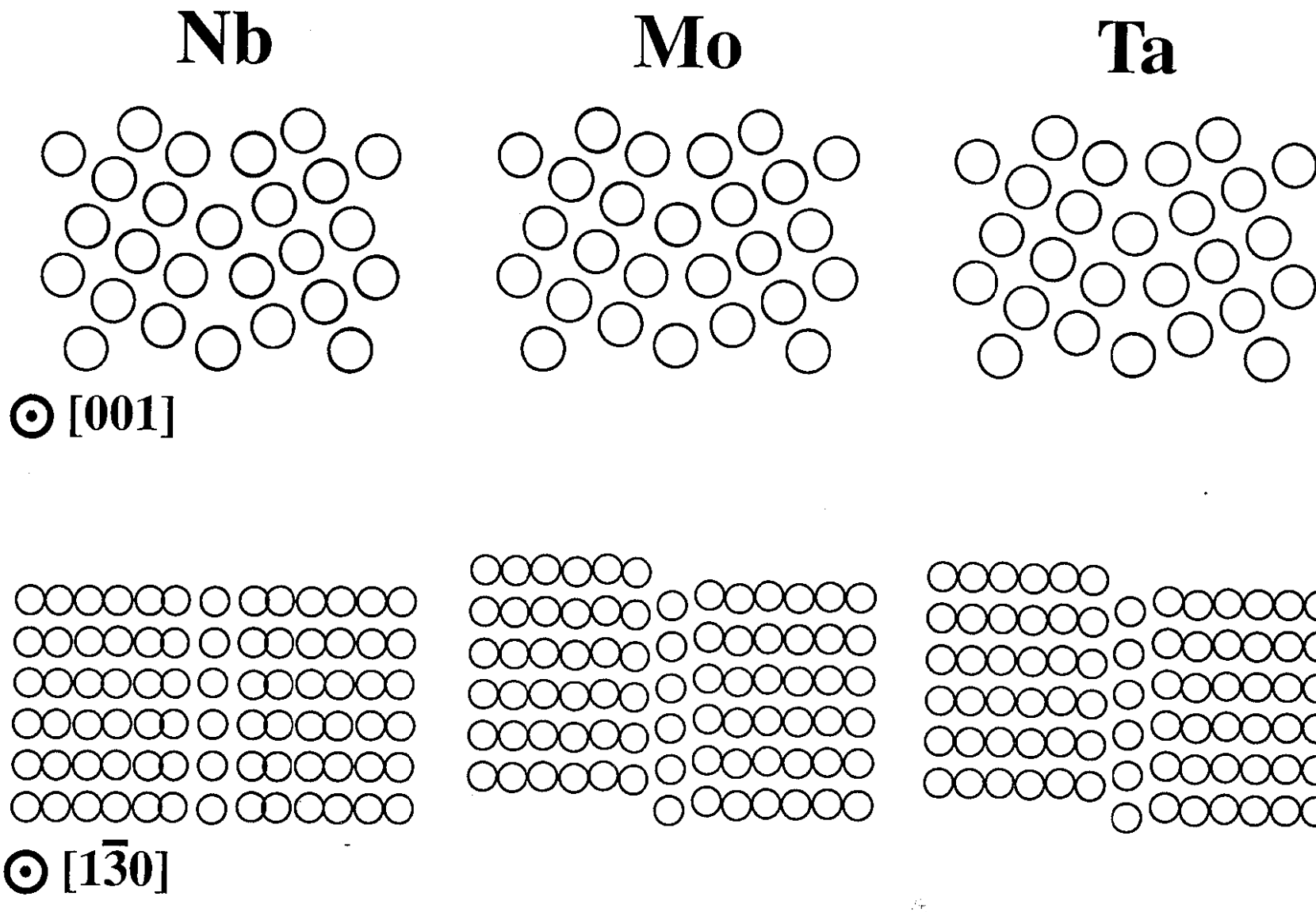

FIG. 3

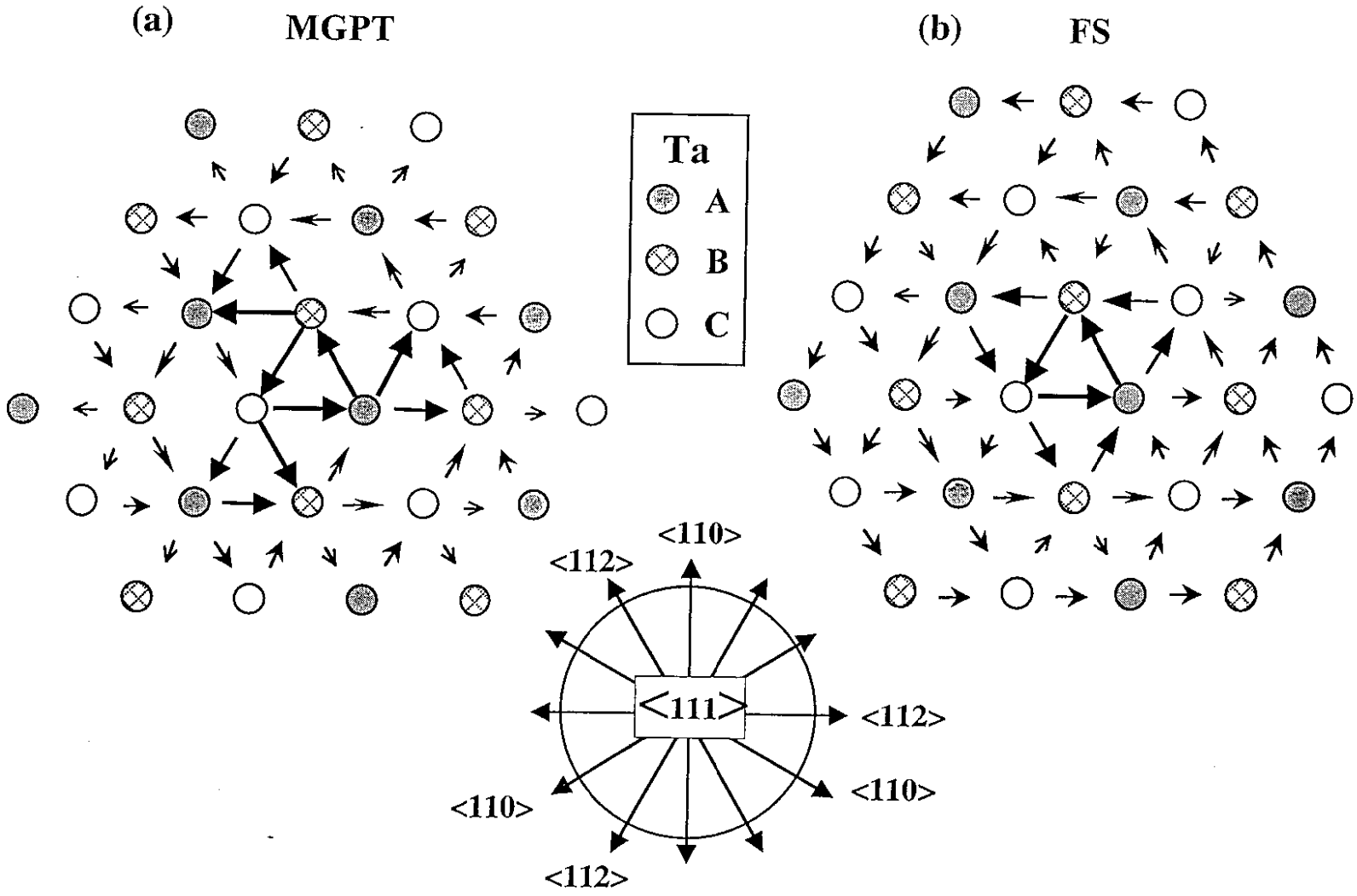
(a)
MGPT
(b)
FS
Ta
A
B
C
<110>
<112>
<111>
<112>
<110>
<110>
<112>

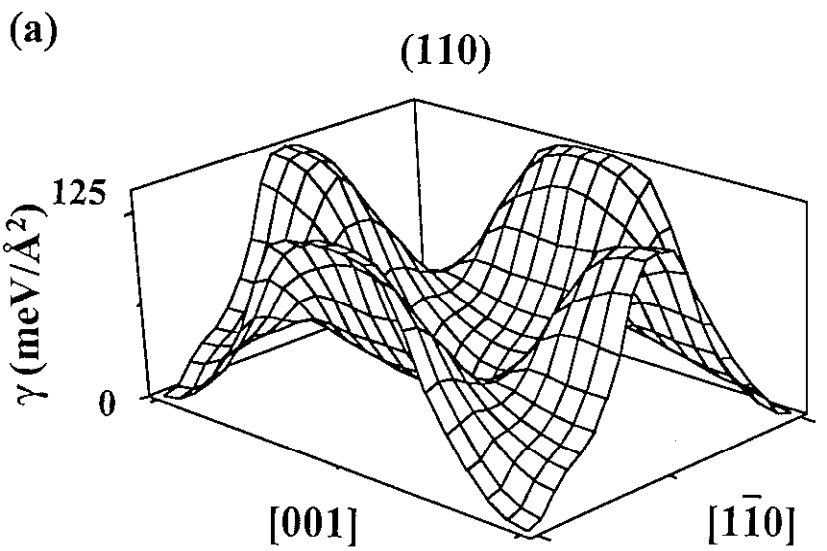
(a)
(110)
125
0
γ (meV/Å²)
[001]
[1$\bar{1}$0]

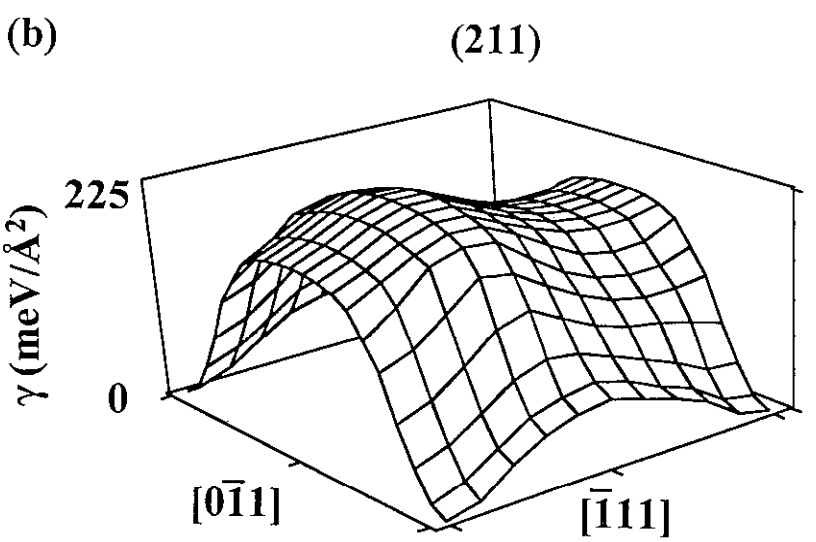
(b)
(211)
225
0
γ (meV/Å²)
[0$\bar{1}$1]
[$\bar{1}$11]

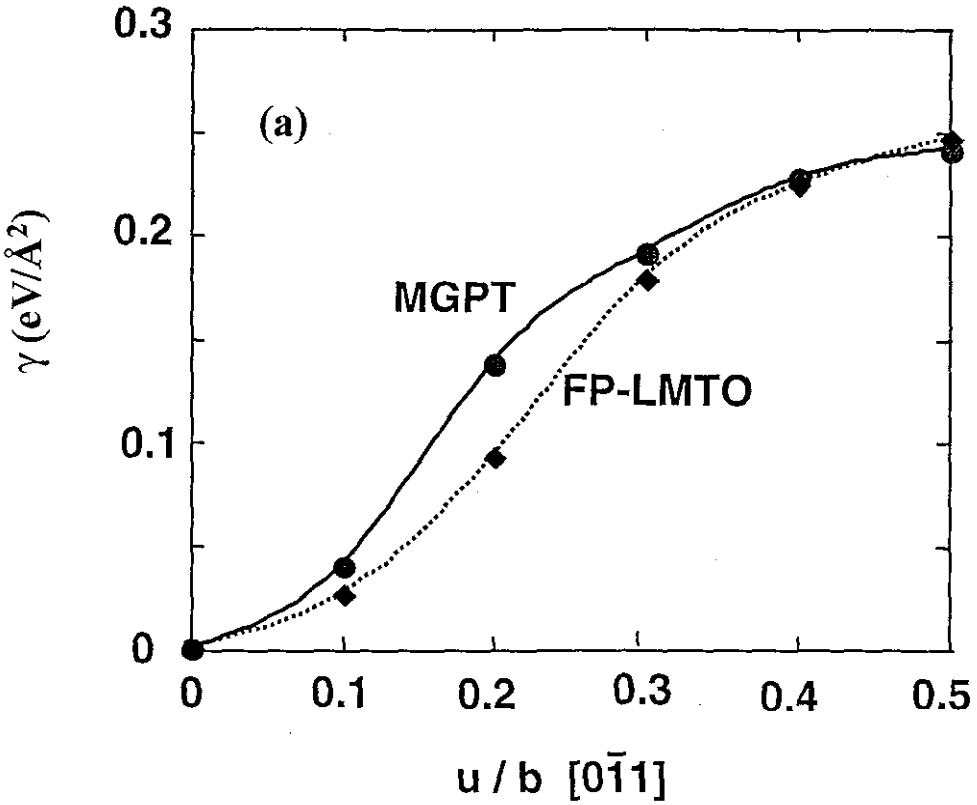
(a)
MGPT
FP-LMTO
γ (eV/Å²)
0.3
0.2
0.1
0
0
0.1
0.2
0.3
0.4
0.5
u / b [0$\bar{1}$1]

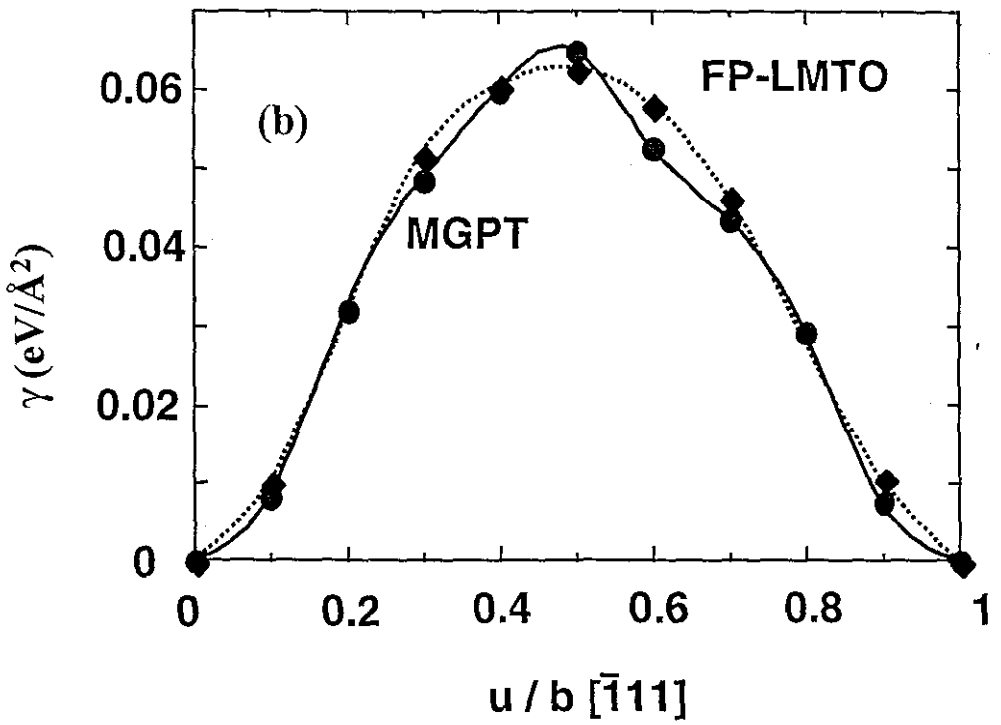
(b)
FP-LMTO
MGPT
γ (eV/Å²)
0.06
0.04
0.02
0
0
0.2
0.4
0.6
0.8
1
u / b [$\bar{1}$11]

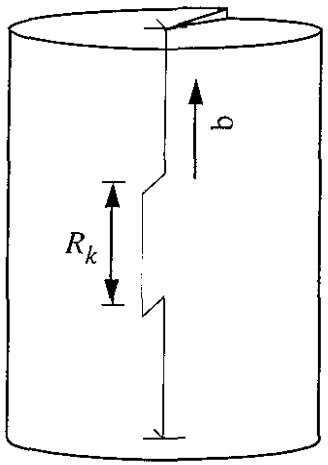

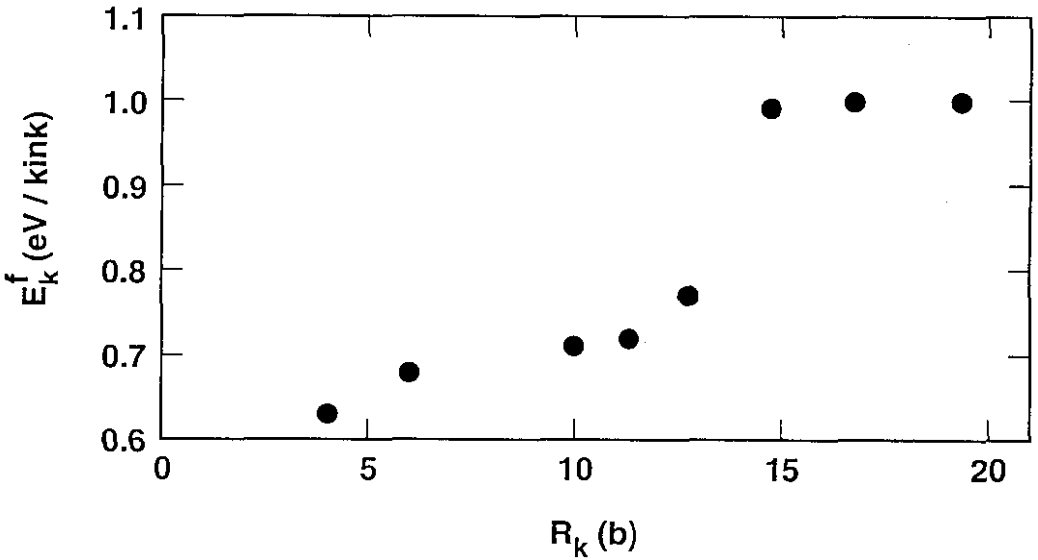

FIG. 7

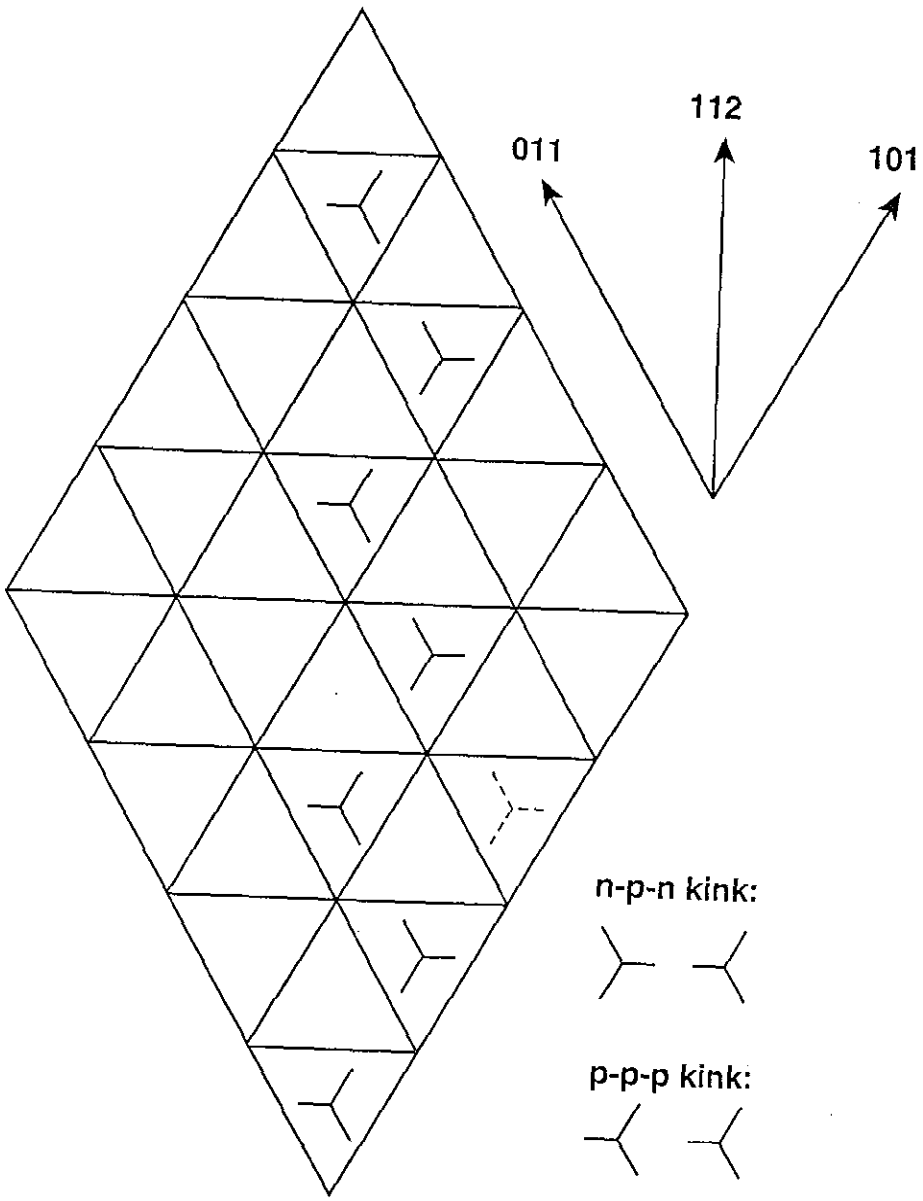
112
011
101
n-p-n kink:
p-p-p kink: